Sodium channels as gateable non-photonic sensors for membrane-delimited reactive species

CrossMark

Navin K. Ojha [a,1], Ehsan Nematian-Ardestani [a,1], Sophie Neugebauer [a], Benjamin Borowski [a], Ahmed El-Hussein [a,b], Toshinori Hoshi [c], Enrico Leipold [a], Stefan H. Heinemann [a,*]

[a] Center for Molecular Biomedicine, Department of Biophysics, Friedrich Schiller University Jena, & Jena University Hospital, Jena, Germany
[b] The National Institute of Laser Enhanced Science, Cairo University, Cairo, Egypt
[c] Department of Physiology, University of Pennsylvania, Philadelphia, USA

ARTICLE INFO

ABSTRACT

Reactive oxygen species (ROS) and reactive oxygen intermediates (ROI) play crucial roles in physiological processes. While excessive ROS damages cells, small fluctuations in ROS levels represent physiological signals important for vital functions. Despite the physiological importance of ROS, many fundamental questions remain unanswered, such as which types of ROS occur in cells, how they distribute inside cells, and how long they remain in an active form. The current study presents a ratiometric sensor of intracellular ROS levels based on genetically engineered voltage-gated sodium channels ($roNa_V$). $roNa_V$ can be used for detecting oxidative modification that occurs near the plasma membrane with a sensitivity similar to existing fluorescence-based ROS sensors. Moreover, $roNa_V$ has several advantages over traditional sensors because it does not need excitation light for sensing, and thus, can be used to detect phototoxic cellular modifications. In addition, the ROS dynamic range of $roNa_V$ is easily manipulated in real time by means of the endogenous channel inactivation mechanism. Measurements on ROS liberated from intracellular Lucifer Yellow and genetically encoded KillerRed have revealed an assessment of ROS lifetime in individual mammalian cells. Flashlight-induced ROS concentration decayed with two major time constants of about 10 and 1000 ms.

© 2014 Elsevier B.V. All rights reserved.

1. Introduction

Reactive species (RS), such as reactive oxygen species (ROS) and reactive oxygen intermediates (ROI), comprise a family of mostly small molecules capable of oxidatively modifying biomolecules such as nucleic acids, proteins, and lipids. Typical ROS are singlet oxygen ($^1O_2$), superoxide ($O_2^{\bullet-}$), hydroxyl (OH•), peroxyl (RO_2•), alkoxyl (RO•) radicals, and hydrogen peroxide (H_2O_2). The major ROS sources endogenous to cells are the mitochondrial respiratory chain and the NADPH oxidases (NOXs). In addition, exogenous sources such as ionizing radiation, UV light, and cigarette smoke contribute to cellular RS exposure. The long-term effects of RS in organisms are often associated with deleterious symptoms such as degenerative diseases and molecular modifications implicated in aging [1,2]. However, RS also serve beneficial roles in the immune system [3] and are now increasingly considered important signaling molecules [4,5].

Given the relevance of RS for numerous physiological and pathophysiological processes, it is essential to understand the molecular mechanisms of their generation, distribution, and function. This, however, requires the precise real-time assessment of their concentrations and/or activities. For this purpose a number of fluorescent dyes have been developed in the past to report on intracellular oxidation events by changing fluorescent properties (for review see [6]). A prominent example is H_2DCF (dihydrodichlorofluorescein), a non-fluorescent low-molecular weight compound that is oxidized to the fluorescent DCF (dichlorofluorescein) when exposed to select reactive species. However, DCF cannot be targeted to specific cellular compartments, and its modification requires a Fenton reaction involving transition metals or an enzymatically driven process [7]. Therefore, genetically encoded RS-sensitive dyes have become very important tools. For example, mutants of the green fluorescent protein (GFP), in which the formation and breakage of a disulfide bridge result in spectral changes (e.g., roGFP2 [8]), bear many advantages such as potentially high sensitivity towards changes in the redox milieu and the option for subcellular targeting. Moreover, owing to two absorption maxima, roGFP2 yields a ratiometric fluorescent signal providing an optical readout that is independent of the concentration of the fluorescent probe itself. The sensitivity and dynamics of roGFP2 have been increased further by fusing it to glutaredoxin-1 allowing real-time imaging of the intracellular redox

* Corresponding author at: Center for Molecular Biomedicine, Department of Biophysics, Friedrich Schiller University Jena & Jena University Hospital, Hans-Knöll-Str. 2, D-07745 Jena, Germany. Tel.: +49 3641 9 39 56 50; fax: +49 3641 9 39 56 52.
E-mail address: Stefan.H.Heinemann@uni-jena.de (S.H. Heinemann).
[1] Both authors contributed equally.

potential [9]. Fusion of the bacterial protein OxyR with yellow fluorescent protein has led to the hydrogen peroxide-sensitive fluorescent probe HyPer [10].

Despite these advances, there is still a great need for RS sensors with optimized or specialized features. In the first place, all RS sensors named so far rely on the excitation with light to read-out the fluorescence; cells will be exposed to photons potentially generating RS and, hence, leading to phototoxicity. Intensity-dependent light-induced DNA damage can activate repair, or even apoptotic, pathways that fundamentally alter the cellular context in which an experiment is being performed. During experiments, repeated exposure to even low levels of UV light can affect the cellular system under investigation. Even visible (blue) light can exert deleterious effects as excitation of endogenous flavins may produce RS with adverse consequences [11]. Moreover, even when targeted to the plasma membrane, detection of RS-related processes directly at the membrane is technically very challenging. Currently available molecular RS sensors are not suited for single-molecule measurements and, last but not least, conventional RS sensors are always active, i.e. they cannot easily be employed for complex kinetic analyses.

The present work introduces an RS sensor based on a voltage-gated sodium (Na$_V$) channel that overcomes some of the limitations listed above. Na$_V$ channels are large membrane proteins that conduct Na$^+$ upon membrane depolarization, primarily to initiate action potentials in neurons and muscle cells. Voltage-dependent activation (channel opening) occurs in about 100 μs upon membrane depolarization; it is followed by spontaneous closure of the channel within about 1 ms, a process referred to as inactivation. Both processes together yield a transient Na$^+$ inward current, in which the degree of inactivation after a certain time can be experimentally assessed with electrophysiological methods.

The Na$_V$ channel protein consists of about 2000 amino-acid residues, organized in four homologous domains, each of which has six transmembrane segments (S1–S6) (Fig. 1a). Every domain harbors a pore/ gate domain (S5–S6) and a voltage-sensing domain (S1–S4). The cytosolic linker between domains III and IV mediates rapid channel

inactivation, where the conserved inactivation motif IFM (isoleucine– phenylalanine–methionine) is of prime importance [12]. Although the structural details are not yet understood, voltage-dependent translocation of the voltage-sensor domains is followed by a conformational change of the DIII–DIV linker with the effect that the IFM motif obstructs the permeation pathway and, hence, terminates Na$^+$ flow [13–15]. Oxidative modification of the methionine within the IFM motif (e.g., formation of methionine sulfoxide) results in a marked loss of inactivation that can be monitored in real time and with high precision by repeatedly recording currents mediated by Na$_V$ channels using whole-cell patch-clamp technology [16]. Introduction of cysteine residues in this motif strongly enhances the sensitivity towards chemical modification [17,18].

Based on these properties, principally allowing for non-photonic ratiometric determination of oxidative reactions right at the plasma membrane, we equipped Na$_V$ channels with cysteine residues in the inactivation motif to yield membrane-based RS sensors. The engineered Na$_V$ channel most suitable as a cellular RS sensor with the mutated motif IFC (roNa$_V$) is characterized in detail, functionally compared with roGFP2, and used to determine dynamics and lifetime of RS in single living cells.

2. Materials and methods

2.1. Expression plasmids and mutagenesis

The wild-type Na$^+$ channel construct used in this study was based on rat Na$_V$1.4 (SCN4A, P15390 [19]) in the plasmid vector pcDNA3. Mutants thereof were generated by site-directed mutagenesis and verified by DNA sequencing (also see [16]). Point mutants were introduced into the inactivation motif 1303IFM (Fig. 1a) and thus mutants are termed by this motif only, e.g. "IFC" for mutant M1305C. In addition, all Na$_V$ channel constructs carried mutation M1316L to remove the potentially oxidation sensitive methionine in the inactivation linker. roGFP2 [8] and CD8 were on pcDNA3 plasmids. The genetically encoded photosensitizer KillerRed was from Evrogen (Moscow, Russia).

2.2. Cell culture

HEK 293 cells (CAMR, Porton Down, Salisbury, UK) were maintained in Dulbecco's Modified Eagle's Medium (DMEM) mixed 1:1 with Ham's F12 medium and supplemented with 10% fetal calf serum in a 5% CO$_2$ incubator. Cells were trypsinized, diluted with culture medium, and grown in 35-mm dishes. Electrophysiological experiments were performed 1–5 days after plating. HEK 293 cells were transfected with the respective plasmids using the Rotifect® transfection reagent (Roth, Karlsruhe, Germany) following the instructions of the supplier. Cells not expressing roGFP2 were cotransfected with CD8 to identify transfected cells by means of anti-CD8-coated beads (Deutsche Dynal GmbH, Hamburg, Germany).

2.3. Electrophysiological measurements

Whole-cell voltage-clamp experiments were performed as described previously [20]. Briefly, patch pipettes with resistances of 0.7– 1.5 MΩ were used. The series resistance was compensated for by more than 70% in order to minimize voltage errors. Perforated-patch clamp recordings were performed by adding escin at 1–10 μM [21] to the patch pipette solution yielding a series resistance between 3 and 20 MΩ after about 15 min in the on-cell configuration.

A patch-clamp amplifier EPC9 was operated by PatchMaster software (both HEKA Elektronik, Lambrecht, Germany). Holding potential was −120 mV. Leak and capacitive currents were corrected with a $p/4$ method with a leak holding voltage of −120 mV. Currents were low-pass filtered at 5 kHz and sampled at a rate of 25 kHz. All experiments were performed at a constant temperature of 19–21 °C.
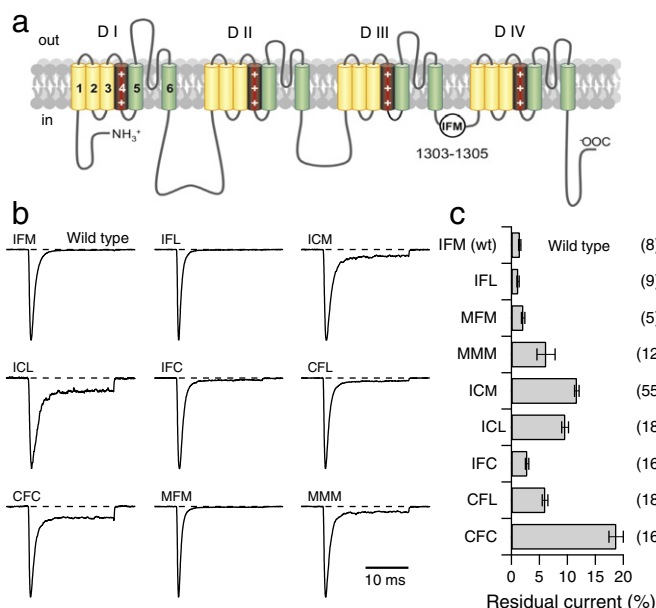

Fig. 1. Properties of point mutants. a) Transmembrane topology of a sodium channel α-subunit highlighting the inactivation motif "IFM". Numbers refer to rat Na$_V$1.4. b) Normalized current responses of Na$_V$1.4 wild type (IFM) and the indicated mutants expressed in HEK 293 cells in response to depolarizations to −20 mV from a holding voltage of −120 mV. c) The residual current at the end of the 20-ms depolarizing pulse relative to the peak current for the indicated mutants. Mean ± SEM (n is shown in parentheses).

The patch pipettes contained (mM): 35 NaCl, 105 CsF, 10 EGTA, and 10 HEPES (pH 7.4 with CsOH). The bath solution contained (mM): 150 NaCl, 2 KCl, 1.5 CaCl$_2$, 1 MgCl$_2$, and 10 HEPES (pH 7.4 with NaOH).

2.4. RS generation

Chloramine-T (ChT) was diluted in the respective bath solution immediately before application. The oxidant was applied extracellularly by exchanging the entire bath volume. Alternatively, cells were loaded with the fluorescent dye Lucifer Yellow (LY) (1 mM; Sigma) via the patch pipette; after recording control currents, cells were illuminated with 436-nm light from a PolyChrome-1 light source (XBO lamp, TILL Photonics, Gräfelfing, Germany) using a 40× dry objective. In some experiments, RS were generated solely by epifluorescence excitation light. This was achieved with light from a monochromator (see above) using a 63×/1.25 oil objective. Alternatively, excitation light of a mercury arc lamp (100-W) was passed through an epifluorescence filter set: GFP, BP 450–490, FT 510 (LP 515); KillerRed, BP 510–560, FT 580 (LP 590), in both cases using a 20×/0.30 dry objective. Rapid RS production was achieved by Xe-lamp flash stimulation (UV-flash, TILL Photonics).

2.5. ROS detection with roGFP2

Fluorescence of individual cells expressing roGFP2 was measured with a photodiode (TILL Photonics). Excitation light of 400 and 475 nm or 465 nm (width about 10 nm) from a PolyChrome-1 light source (TILL Photonics) was applied for 20 ms each. Fluorescence ratio (F400/F475) was formed based on the mean fluorescence values of the trailing 10-ms intervals. Filter set: 492/SP, FT 495, and HC 520/35 (AHF Analysentechnik, Tübingen, Germany).

2.6. Current–voltage relationships

From a holding potential of −120 mV, cells were depolarized to −80 through 60 mV in steps of 10 mV for 40 ms every 3 s. The peak current–voltage relationships were fit according to a Hodgkin–Huxley formalism with $m = 3$ activation gates and a single-channel conductance according to the Goldman–Hodgkin–Katz equation.

$$I(V) = \Gamma V \frac{1 - e^{-(V - E_{rev})/25mV}}{1 - e^{-V/25mV}} \frac{1}{\left(1 + e^{-(V - V_m)/k_m}\right)^3} \quad (1)$$

V_m is the voltage of half-maximal gate activation and k_m is the corresponding slope factor. Γ is the maximal conductance of all channels and E_{rev} is the reversal potential.

2.7. Voltage dependence of fast inactivation

From a holding potential of −120 mV, cells were conditioned for 500 ms at voltages ranging from −140 to 0 mV in steps of 5 mV. Subsequently, peak current was determined at −10 mV and normalized to a control peak current measured before conditioning. The repetition interval was 3 s. The normalized peak current plotted versus the conditioning voltage was described with a Boltzmann function:

$$\frac{I(V)}{I_{contr}} = \frac{1}{1 + e^{-(V - V_h)/k_h}} \quad (2)$$

with the half-maximal inactivation voltage, V_h, and the corresponding slope factor, k_h, which indicates the voltage dependence of inactivation.

2.8. Time course of inactivation removal

The time course of oxidation-induced loss of inactivation was monitored by measuring the ratio of current at 5 ms (I_5) or 10 ms (I_{10}) after

the depolarization onset and the peak current (I_p) elicited by pulses to −20 mV (r). The inactivation index, $1-r(t)$, was plotted as a function of time (t) and fit with the following function:

$$1 - r(t) = 1 - r_0 - (r_\infty - r_0)\left(1 - e^{-(t - t_0)/\tau}\right)^n \quad (3)$$

with the ratio before oxidation, r_0, the time of oxidation start, t_0, the time constant, τ, and an exponent, n. r_∞ is the ratio after infinite oxidation.

2.9. Data analysis and statistics

Data were analyzed with FitMaster (HEKA Elektronik) and IgorPro (WaveMetrics, Lake Oswego, OR, USA) software. Averaged data are presented as mean ± SEM ($n =$ number of independent measurements). Groups of data were compared with a two-sided Student's t-test followed by a *post hoc* Bonferroni correction when appropriate.

3. Results

3.1. Selection of a ROS-sensitive sodium channel mutant

The rapid inactivation of voltage-gated sodium channels is mainly mediated by the inactivation motif "IFM" (Ile-Phe-Met), located in the intracellular linker between domains III and IV (Fig. 1a) [12]. In a previous study [16] we showed that exposure of Na$_V$ channels to the oxidant chloramine T (ChT) efficiently removes rapid inactivation, mainly via chemical modification of the methionine residue in the inactivation motif (Met1305 for rat Na$_V$1.4). Thus, we hypothesized that introduction of either additional Met residues or Cys residues in the inactivation motif might make the inactivation even more susceptible to oxidative modification. Hence, several single- or double-site mutants with either Met or Cys were generated. Such mutants were expressed in HEK 293 cells and their function was evaluated by means of the whole-cell patch-clamp method. As illustrated in SFig. 1, such mutants exhibited only marginal alterations with respect to their voltage dependence of activation (SFig. 1a). Voltage dependence of inactivation was most strongly affected in mutants ICL und CFC (SFig. 1b). For an application of one of these mutants as an RS sensor, a voltage dependence of activation and inactivation close to the wild type would be desirable; in addition, rapid inactivation should be nearly complete as to avoid Na$^+$ influx into cells under sustained depolarization. We thus analyzed the time course of inactivation at −20 mV and the fraction of steady-state current at that potential. As shown in Fig. 1b and c, all mutants with additional Met or Cys residues exhibit a greater steady-state current than the wild type (IFM). Among them, the inactivation time courses of mutants MFM and IFC were most similar to that of the wild type. Application of the reducing agent DTT did not decrease the fractional steady-state current in IFC further, indicating that incomplete inactivation is not caused by oxidation of the introduced cysteine residue under control conditions. Recovery from inactivation was similar or even faster than the wild type for all mutants tested (SFig. 1c).

All of the mutants with additional Cys residues were then subjected to 50 μM ChT, and those with an altered number of Met residues were exposed to 500 μM ChT. All mutants carrying a Cys residue lost inactivation on ChT exposure with single-exponential time course characterized by time constants of 50–70 s, while the wild type showed a very small response only (Fig. 2a, b, d). ChT at ten-times higher concentration removed inactivation of the wild type with a time constant of about 300 s, while an increasing number of Met residues accelerated that process (MFM, about 60 s; MMM, about 30 s); mutant IFL served as a negative control (Fig. 2c, e).

These results indicate that a Cys residue at any position within the IFM motif results in channels with strongly RS-sensitive inactivation. Since a mutant with the least steady-state current under control
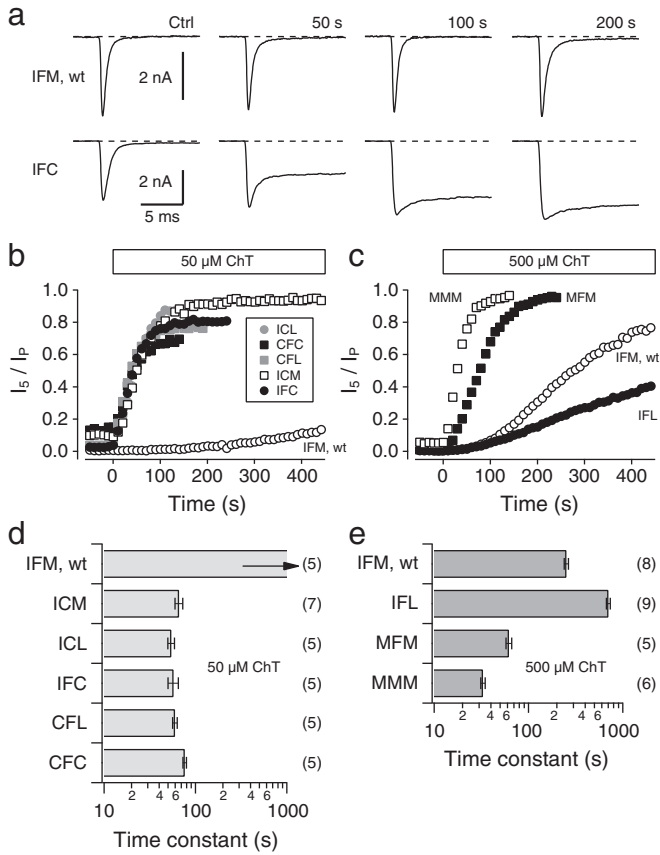
Fig. 2. Removal of fast inactivation by chloramine T (ChT). a) Current traces at −20 mV for Na$_V$1.4 wild type (IFM, top) and mutant IFC (bottom) in HEK 293 cells before (Ctrl) and after (time indicated) application of 50 μM ChT. b) Time course of inactivation removal in response to application of 50 μM ChT for the wild type and the indicated cysteine mutants. c) Time course of inactivation removal in response to application of 500 μM ChT for the wild type and the indicated methionine mutants. Mutant IFL served as a negative control. d, e) Time constants for inactivation removal for the indicated channels in response to 50 μM ChT (d) and 500 μM ChT (e). Mean ± SEM (n is shown in parentheses).

conditions (Fig. 1b, c) was most desirable, we selected mutant IFC for further analysis. If Met-directed modifications were to be studied, mutants MFM and MMM are both suited.

3.2. Characterization of mutant IFC

The potential usefulness of mutant IFC as a sensor for ChT-induced modification is shown in Fig. 3. The kinetics of inactivation loss upon ChT application to transiently transfected HEK 293 cells was estimated with single-exponential functions for various ChT concentrations. The inverse of the time constant, i.e. "$k_{on} + c\,k_{off}$" assuming a first-order reaction, is plotted in Fig. 3a. The superimposed fit is a result assuming $k_{off} = 0$, i.e., an irreversible reaction, yielding a forward rate constant of $382 \pm 21\ \mathrm{s^{-1}\,M^{-1}}$, suggesting that IFC can be used to detect ChT-induced chemical modifications down to about 500 nM. The assumption of $k_{off} = 0$ is reasonable because the loss of inactivation exerted by short exposure to ChT remained stable when ChT was washed away (Fig. 3b). The process studied so far is of physiological relevance because the reaction is reversible provided there are reducing conditions. As shown in Fig. 3c, inactivation of mutant IFC was partially removed by short exposure to 5 μM ChT. Subsequently, the bath was washed with extracellular saline containing 1 mM DTT; DTT completely restored inactivation with a time constant of about 1000 s. To further confirm that ChT mediates its effect via a redox process, we measured the kinetics of inactivation loss induced with 3 μM ChT under control conditions and with the non-specific ROS scavenger ascorbic acid
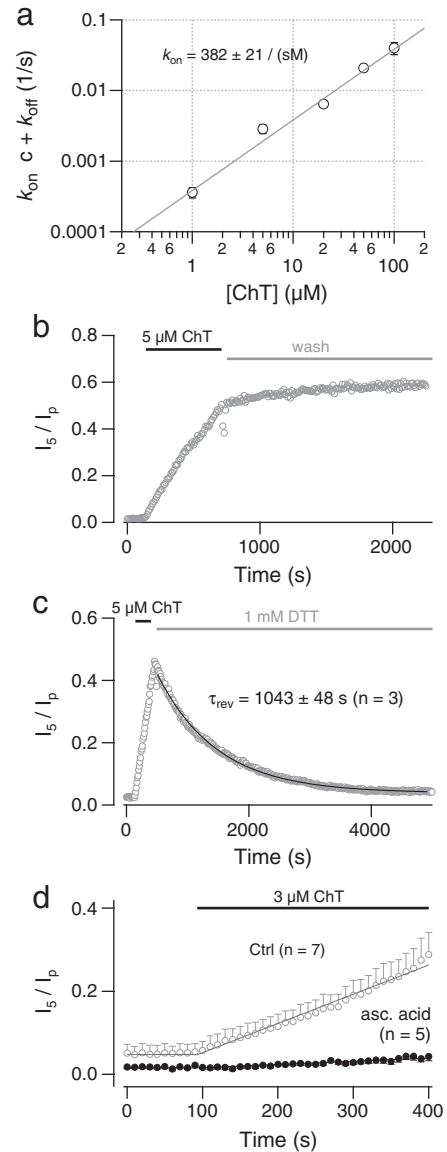

Fig. 3. Concentration dependence and reversibility of mutant IFC. a) Inverse of the time constant of onset of inactivation removal for mutant IFC in response to application of ChT at various concentrations. The straight line is a fit according to a first-order binding with no reversibility ($k_{off} = 0$) yielding an on-rate of $k_{on} = 382 \pm 21$/s/M. b, c) Representative experiments showing the ChT-induced removal of inactivation that persists when ChT is washed out (b) or is restored upon application of bath solution containing DTT (1 mM), c). The time constant of recovery upon DTT application was 1043 ± 48 s ($n = 3$); a_0–a_1 values (before ChT/after DTT) were: =1.8/2.0%; 3.9/2.5%; 8.6/10.0%. d) Application of 3 μM ChT under control conditions and with 2 mM ascorbic acid supplemented to the pipette solution. Mean ± SEM ($n = 7$ and 5). The superimposed curves are linear functions starting at the beginning of ChT application with slopes of $70.3 \pm 1.16\ 10^{-5}$/s (Ctrl) and $7.74 \pm 0.44\ 10^{-5}$/s (ascorbic acid).

(2 mM) supplemented to the patch pipette solution. As shown in Fig. 3d, in the presence of intracellular ascorbic acid the effect of extracellularly applied ChT was about 10-times weaker (linear slope changed by a factor of 0.110 ± 0.007).

3.3. Comparison of mutant IFC with roGFP2

Changes in the intracellular redox milieu are often inferred using variants of the green fluorescence protein (GFP) in which extra cysteine residues are introduced (roGFP2 [8]). The ROS sensitivities of roGFP2 and mutant IFC were compared by coexpressing both in HEK 293 cells and measuring Na$^+$ currents in the whole-cell configuration in parallel

to recording fluorescence of the same cell. Channels were activated every second with a 20-ms depolarization to −20 mV. Simultaneously, excitation light of 400 and 475 nm (20 ms each) was applied (Fig. 4a). Inactivation of mutant IFC was judged by the ratio I_{10}/I_p while the state of roGFP2 was measured as F400/F475. The time course of the signals in a representative cell is shown in Fig. 4b, illustrating three differences between the IFC signal and the roGFP signal: (1) while I_{10}/I_p was stable before ChT application, F400/F475 slightly increased; (2) the overall dynamic range of the ratiometric signals was about 0.8 for I_{10}/I_p, while that of F400/F475 was only about 0.2; (3) the channel signal increased much more quickly than the roGFP2 signal upon stimulation. The latter was estimated by a linear fit of the initial 20 s upon stimulation with 50 µM ChT yielding slopes in the ratios of 0.0177 ± 0026 for the channel and 0.0016 ± 0.0003 for roGFP2 ($n = 6$, $P = 0.0015$). Thus, the ratiometric RS-related signal derived from mutant IFC responds about 10-times faster to ChT application than roGFP2. Both signals saturate after about 100–200 s. Given its useful properties, the modified sodium channel $Na_V1.4$ with an IFC motif in the inactivation domain is hereafter referred to as $roNa_V$.

3.4. Detection of light-induced RS with roNa_V

Although the use of roGFP2 or other related genetically encoded or synthetic optical reporters is convenient, their application is limited to situations where the excitation light itself is not a confounding factor. However, if light is an integral part of an experiment, light-independent detection of RS in single cells may be desirable. We thus assayed the usefulness of $roNa_V$ to detect photodamage induced by excitation light in an epifluorescence setting. Wild-type and $roNa_V$ channels were expressed in HEK 293 cells and currents were recorded in the whole-cell configuration. Cells were placed into the focus of a $20\times$ dry objective of an inverted microscope with a 100-W mercury lamp for epifluorescence excitation. After several control recordings in the dark, light was turned on and the
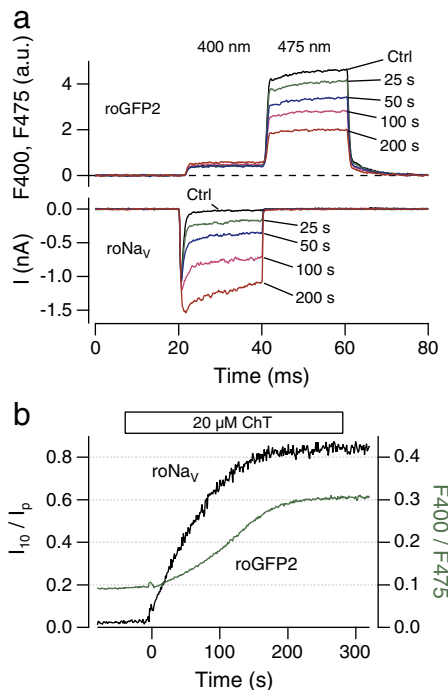
loss of inactivation was monitored. Excitation through a filter set commonly used for GFP detection (BP 450–490, FT 510), i.e. stimulating with blue light, resulted in rapid progressive loss of $roNa_V$ inactivation, while the effect in the wild type was much smaller (Fig. 5a, b). Even excitation with green light (BP 510–560, FT 580) noticeably removed inactivation in $roNa_V$ with only marginal effects on the wild type (Fig. 5c, d). Thus, $roNa_V$ is a useful tool for detecting RS generated by cell exposure to light. The sensitivity is high enough to even monitor functional changes induced by RS originating from green light (510–560 nm). Under similar conditions, RS-sensitive fluorescent dyes may bleach. Moreover, the use of roGFP to measure RS is not feasible without the generation of RS by the required excitation light.

3.5. Gated RS sensitivity of roNa_V

To infer about the dynamics of RS distribution and lifetime, a sensor that responds to RS in a reversible manner is required. Sensors relying on the formation of disulfide bridges to report on the redox state (like roGFP2) may not be suited because, depending on the reactive species, cysteines will be modified in an irreversible manner, for example to sulfinic or sulfonic acid, thus disabling the sensor. One solution to this problem would be to develop an RS sensor that can be turned on and off at will to take snapshots of intracellular RS activity (or concentration). Ion channels are molecular switches par excellence, in particular voltage-gated sodium channels that open and close in response to changes in membrane voltage in the millisecond range. Since the RS-sensitive element in $roNa_V$ is the cysteine in the inactivation motif, we hypothesized that the motif is protected from RS attack when it is in the inactivated state, i.e. forming a firm contact with the channel protein. At resting conditions, the IFC motif is expected to be readily
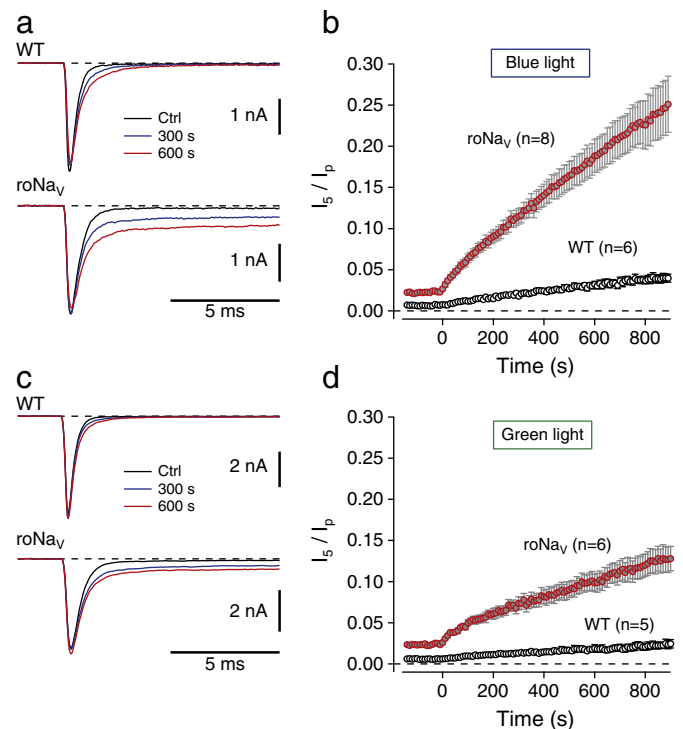

Fig. 4. Comparison of mutant IFC ($roNa_V$) with roGFP2. a) Raw data traces of single-cell fluorescence with excitation pulses at 400 and 475 nm (*top*) and current responses at −20 mV of the same cell (*bottom*), expressing mutant IFC. Data were recorded before (Ctrl) and after application of 20 µM ChT to the bath solutions. Time of measurement is indicated. b) Time courses of the loss of inactivation (I_{10}/I_p, black) and the ratio F400/F475 of roGFP2 fluorescence in response to ChT application.

Fig. 5. Photodamage induced by illumination typically employed in epifluorescence experiments. a) Raw data traces in response to depolarizations to −10 mV for the wild type (*top*) and mutant IFC ($roNa_V$, *bottom*) before (Ctrl) and 300 and 600 s after epifluorescence excitation light were turned on. 100-W mercury lamp, BP 450–490, FT 510, $20\times/0.30$ Ph1 dry LD A-Plan, 8.3 mW objective output measured at 470 nm. b) Time course of mean inactivation loss on light exposure; error bars indicate SEM values. c, d) similar to a and b but using green light instead of blue light: BP 510–560, FT 580, 32 mW objective output measured at 535 nm.

accessible to the cytosolic solution and susceptible to RS-induced modification.

Experimental protocols were devised to test for a "state dependence" of roNa$_V$'s RS sensitivity. If the sensor is completely protected from RS in the inactivated state, one would expect a slowing down of the RS-induced loss of inactivation proportional to the time spent in the inactivated state. In the experiment shown in Fig. 6a, b, loss of inactivation in response to 10 μM ChT application was measured under control conditions, i.e. holding voltage of −120 mV and test pulses every 15.6 s. Using this protocol, loss of inactivation proceeded with a time constant of 230 s. In the protocol that contained 10-s episodes at −50 mV to inactivate most of the channels, the time constant increased to 486 s. Assuming an irreversible first-order reaction, this yields reaction rates of 4.35/ms and 2.02/ms, respectively. If we further assume that the channels are totally insensitive when they are in the inactivated state, a lower limit for the reaction rate for the second protocol is 4.35/ms * (15.6–10.0)/15.6 = 1.56/ms. Thus, the measured rate of

2.02/ms comes close to this limit arguing for an almost perfect protection of the IFC motif in the inactivated state.

A likely explanation for the effect described could be a limited access of ChT to the site of action rather than a restricted access of RS. Therefore, three other means of RS generation were tested, all triggered by light. In addition, it was desirable to use repetitively the same electrophysiological pulse protocol in order to avoid any confounding impact of slow channel inactivation. In a first example, cells expressing roGFP2 and roNa$_V$ were subjected to 400-nm light and assayed for the ratiometric ROS-related signal every 5 s. While the resting holding potential was −120 mV, light resulted in a progressive loss of inactivation and a ROS-signal detected by roGFP2. During an episode with a holding potential of −20 mV, roNa$_V$ was inactivated and unavailable for measurements while roGFP2 proceeded to become modified. Resuming a holding potential of −120 mV indicated that, upon a phase necessary to recover from inactivation, roNa$_V$ was effectively protected from modification during the −20-mV episode (Fig. 6c). Similar assays with equivalent results were performed in the perforated-patch configuration thus preserving the cytosol and supporting the usefulness of roNa$_V$ (SFig. 2).

In a second example we loaded the cell via the patch pipette with Lucifer Yellow, a commonly used fluorescent dye that produces ROS upon irradiation [16,22] and stimulated with blue light (SFig. 3a–c). In a third example we expressed the genetically encoded photosensitizer KillerRed [23] together with roNa$_V$ in HEK 293 cells and stimulated RS production with green light (SFig. 3d). In both cases we assayed the incremental loss of roNa$_V$ inactivation depending on whether the light pulse was given during the resting state (−120 mV) or during an inactivation episode (−50 mV) and also confirmed for these RS sources that roNa$_V$ exhibits properties of a gateable RS-sensitive sensor that can be protected from RS reactions by switching the channel into an inactivated state.

3.6. Dynamics of intracellular RS monitored with roNa$_V$

If strong RS sources are to be evaluated, the lifetime of RS can be measured by directly observing the reaction kinetics with roNa$_V$. Since roNa$_V$ inactivates in about 5 ms and a period of about 10 ms is required to fully recover roNa$_V$ from fast inactivation, one should be able to monitor the state of roNa$_V$ with a sample interval of about 15 ms. If a singular RS-production event is considered, the time resolution can be even higher by tuning the delay between RS production and roNa$_V$-mediated readout. We therefore selected Lucifer Yellow as a source for rapid RS production and illuminated the cells with brief light flashes with a half-width of about 600 μs. As illustrated in Fig. 7, a single flash event causes a substantial loss of inactivation in the immediately following pulse. Analysis of the time course of roNa$_V$ signals revealed the existence of at least two time constants. Using 5-ms depolarizations at an interval of 25 ms (Fig. 7c), an upper limit of the fast component of about 10 ms was determined. In this fast component about 1/3 of the total modification process occurred; the remaining fraction developed within a process on the order of seconds. This result shows that roNa$_V$ is suited to monitor the lifetime of different light-induced reactive species components acting at the plasma membrane.

4. Discussion

Reactive oxygen species and reactive oxygen intermediates are important signaling molecules in many physiological and pathophysiological processes (e.g. [2,24,25]) and constitute an important factor in cellular aging [1,26]. Therefore, the investigation of RS-associated biological functions and/or deleterious effects on cells and whole organisms requires tools for their monitoring and quantification. However, reactive species present some characteristics that make them difficult to detect, namely their short lifetime and their interaction with a variety of antioxidants existing *in vivo* capable of capturing these reactive
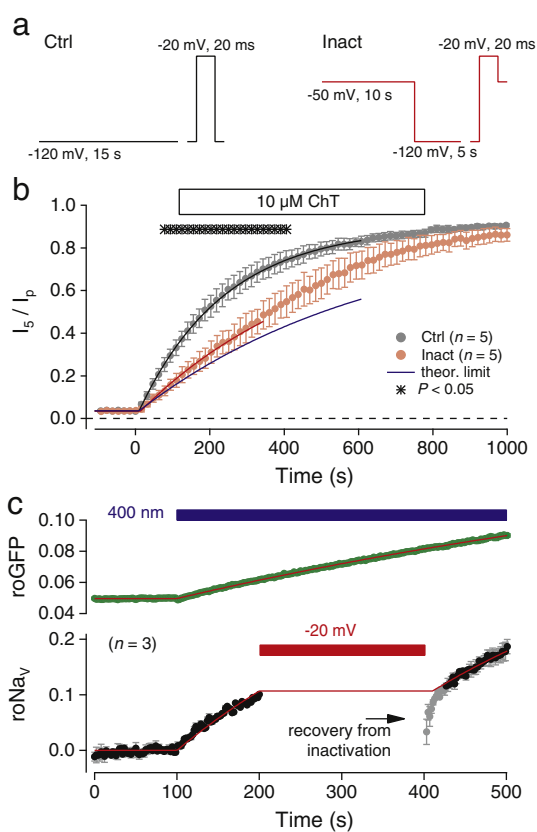

Fig. 6. State dependence of roNa$_V$ modification. a) Pulse protocols used to test for a state dependence of RS-induced loss of inactivation. In the left condition (Ctrl), 20-ms depolarizations to −20 mV were elicited every 15 s with a constant holding voltage of −120 mV. In the protocol on the right (Inact), the first 10 s of the holding period was at −50 mV to inactivate the channels, followed by a 5-s period at −120 mV to ensure full recovery from inactivation before the test pulse to −20 mV was elicited. b) Time courses of loss of inactivation upon application of 10 μM ChT for the control protocol (Ctrl) and the inactivation protocol (Inact). Error bars denote SEM values of $n = 5$ cells each. Also indicated is the statistical evaluation (asterisks, two-sided *t*-test with unequal variances) of the differences between both groups as a function of time. Superimposed to the mean data are single-exponential fits with a limiting ratio of 0.9 to estimate the initial slope of inactivation loss. Ctrl: $\tau = 232 \pm 5.8$ s; Inact: $\tau = 496 \pm 25$ s. The blue curve is a prediction of the time course of modification assuming full protection of the IFC motif during the period of channel inactivation. c) Loss of roNa$_V$ inactivation (*bottom*) and roGFP2 signal (*top*) in response to illuminating a cell with 400-nm light (blue bar). In the episode indicated by the red bar the holding potential was set to −20 mV in order to inactivate the Na$_V$ channels. Superimposed curves indicate mono-exponential time courses of the RS effect; for roNa$_V$, data are described well assuming that no light-induced modification has happened during the inactivation episode.
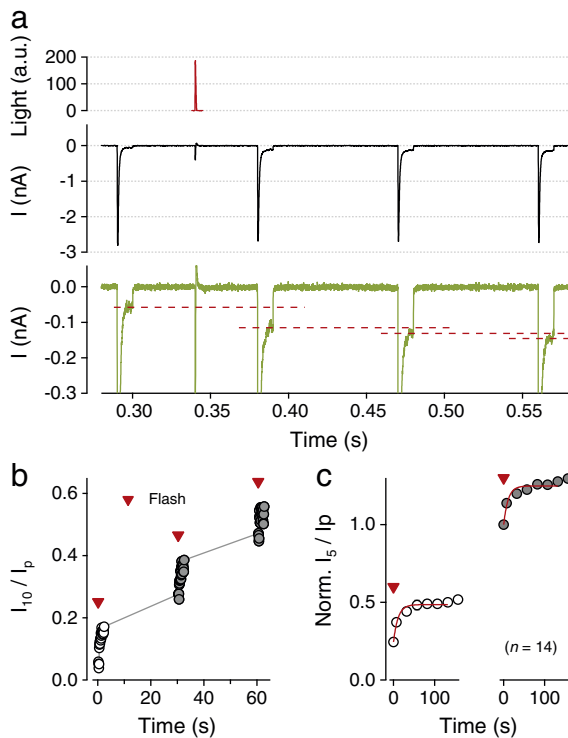
Fig. 7. Kinetics of roNa$_V$ modification by light-induced RS generation. a) (*top*) recording of a light flash stimulation applied to liberate RS from Lucifer Yellow. (*middle*) current trace with 10-ms depolarizations to activate roNa$_V$ every 80 ms, indicating that the flash applied between the first and the second depolarization shown in this panel only slightly reduced the peak current amplitude. (*bottom*) the same data after scaling by a factor of 10 in order to visualize the degree of non-inactivating current. The horizontal dashed lines indicate such current levels and the progressive loss of inactivation from one pulse to the next clearly showing that a great fraction of inactivation loss has happened in the first pulse after the flash, i.e. in less than 40 ms. b) Degree of inactivation removal as a function of time on a longer time scale showing the results of three subsequent trains of depolarizations (each data point refers to one depolarizing pulse) in which a light flash was given for each train after the third depolarization (indicated by red inverted triangles). This time course shows a very rapid initial loss of inactivation (ms range) followed by a slower process with a time constant of more than 1 s. c) Average time course of flash-light induced loss of inactivation for two successive trains of 5-ms depolarizations at an interval of 25 ms. The data are normalized to the inactivation index obtained before the second light flash. The superimposed red curves are single-exponential fits yielding time constants of 11.0 ± 2.2 ms for the first and 10.7 ± 3.2 ms for the second train; the corresponding amplitudes were 0.251 ± 0.008 and 0.248 ± 0.012, respectively.

species [6]. Fluorescent ROS reporters [6] and in particular genetically encoded proteins such as ROS-sensitive green fluorescence protein (roGFP) and variants thereof (e.g. [8,27]) are undoubtedly very useful tools for studying RS signaling in living cells. However, depending on the application, such systems may suffer from various limitations thus requiring the search of alternative methods of cellular RS detection. Here we introduced roNa$_V$, a voltage-gated sodium channel with a cysteine residue in its inactivation motif (IFC instead of IFM) as a plausible alternative to fluorescent dyes. The degree of RS-mediated channel modification is measured as a ratiometric signal from its degree of inactivation, thus yielding a concentration-independent parameter allowing for absolute calibration.

Mutation IFC was selected among several others harboring a cysteine residue inside the inactivation motif "IFM" because of its small residual non-inactivating current under reducing conditions. This means that replacement of cysteine for methionine in the IFM motif only has a minor impact on the stability of the inactivation domain at its receptor site.

The strongest argument for its use comes from the potential phototoxicity of blue light needed to elicit roGFP signals. Light in the wavelength range of 400 to 500 nm, which is required to detect roGFP signals, can be absorbed by endogenous chromophores such as flavins

to produce ROS [11,28], thus strongly impeding the process of ROS detection. Moreover, the effects on cell membrane components induced by seemingly non-destructive short-time exposure to visible light are not fully explored.

Because measurements using roNa$_V$ do not require light, it can be used to study such phototoxic effects. As illustrated in Fig. 5, even light of moderate intensity (20× objective) and long wavelength (≥510 nm) substantially affects the redox state. Therefore, every ROS measurement involving GFP excitation will inherently suffer from the light-induced disturbance of the cell. Moreover, the light independence of roNa$_V$ is an advantageous feature whenever excitation light would interfere with other light-sensitive components. An example of this is the measurement of RS produced by KillerRed (SFig. 3d).

Quantitative comparison of roNa$_V$ with roGFP signals recorded from the same cell and stimulating with various RS sources yielded similar results. roNa$_V$ displays a greater dynamic range but the calculated ratiometric signal is noisier than that for roGFP because peak Na$^+$ current is part of the measurement and, hence, the signal cannot be averaged as much as, for example, fluorescence episodes of 20 ms. Moreover, the roNa$_V$ signal is formed by approximately 1000–10,000 channel proteins only and, thus, is subject to greater statistical fluctuations (non-stationary channel noise).

A very important advantage of roNa$_V$ is that the recorded signal always represents a chemical process occurring right at the plasma membrane. This is an important aspect if membrane-delimited processes are to be studied. In comparison, even membrane-targeted variants of roGFP will not provide a "clean" membrane-delimited signal because of limited spatial resolution of a microscope and typical strong background fluorescence from roGFP molecules elsewhere in the cytosol.

Importantly, we showed that roNa$_V$ can be sent into a "hibernating" state by depolarizing the membrane. Under this condition the channels enter an inactivated state in which the relevant cysteine residue in the IFC motif apparently becomes protected from RS attacks. This was not only true for chloramine-T challenge but also for RS generated via light, light-excited Lucifer Yellow, and via excitation of the genetically encoded ROS-producing protein KillerRed. By designing of tailored pulse protocols one can thus read-out roNa$_V$ only at specific intervals and protect it from RS-mediated destruction otherwise.

The roNa$_V$ method does have some disadvantages: most importantly, the requirement of performing patch-clamp experiments on single cells. This involves a low throughput and full electrophysiological equipment. In addition, the process of "patching" a cell, i.e. establishing a tight contact between the glass pipette and the cell by itself, and by application of pulse protocols necessary to read-out roNa$_V$, may have an impact on the cellular ROS signaling. In addition, one should be aware that in typical whole-cell recordings the cytosol will progressively lose its reducing power because the cellular components will inevitably leave the cell in long recording sessions. An alternative can be the application of the perforated patch method ("slow whole-cell mode") as illustrated in SFig. 2.

Given the fast response time of roNa$_V$ and its independence on light, it can be quite useful in studying distribution and lifetime of reactive species triggered by light pulses. To demonstrate this option, we liberated RS from cell-loaded Lucifer Yellow with brief (600 µs) light flashes. Following this light flash, the time course of roNa$_V$ modification can be followed at a time resolution of a few milliseconds. In our example we showed that RS originating from Lucifer Yellow "decay" in living HEK 293 cells under voltage-clamp control with two time constants: one about 10 ms and the other on the order of seconds. This indicates that at least two major species of reactive components with the respective mean lifetimes are released when Lucifer Yellow is excited with blue light.

The genetically engineered, gateable, ratiometric, light independent, and membrane-based ROS biosensor (roNa$_V$) might be a potential tool for investigating phototoxicity and various biological functions of reactive species, in particular those occurring close to the plasma membrane.

Acknowledgements

Appendix A. Supplementary data

Supplementary data to this article can be found online at http://dx.doi.org/10.1016/j.bbamem.2014.01.031.

References

[1] E.E. Essick, F. Sam, Oxidative stress and autophagy in cardiac disease, neurological disorders, aging and cancer, Oxidative Med. Cell. Longev. 3 (2010) 168–177.
[2] K. Brieger, S. Schiavone, F.J. Miller Jr., K.H. Krause, Reactive oxygen species: from health to disease, Swiss Med. Wkly. 142 (2012) 13659.
[3] J.D. Lambeth, NOX enzymes and the biology of reactive oxygen, Nat. Rev. Immunol. 4 (2004) 181–189.
[4] E.A. Veal, A.M. Day, B.A. Morgan, Hydrogen peroxide sensing and signaling, Mol. Cell 26 (2007) 1–14.
[5] K.A. Kennedy, S.D. Sandiford, I.S. Skerjanc, S.S. Li, Reactive oxygen species and the neuronal fate, Cell. Mol. Life Sci. 69 (2012) 215–221.
[6] A. Gomes, A. Fernandes, J.L.F.C. Lima, Fluorescent probes used for detection of reactive oxygen species, J. Biochem. Biophys. Methods 65 (2005) 45–80.
[7] M. Karlsson, T. Kurz, U.T. Brunk, S.E. Nilsson, C.I. Frennesson, What does the commonly used DCF test for oxidative stress really show? Biochem. J. 428 (2010) 183–190.
[8] C.T. Dooley, T.M. Dore, G.T. Hanson, W.C. Jackson, S.J. Remington, R.Y. Tsien, Imaging dynamic redox changes in mammalian cells with green fluorescent protein indicators, J. Biol. Chem. 279 (2004) 22284–22293.
[9] M. Gutscher, A.L. Pauleau, L. Marty, T. Brach, G.H. Wabnitz, Y. Samstag, A.J. Meyer, T.P. Dick, Real-time imaging of the intracellular glutathione redox potential, Nat. Methods 5 (2008) 553–559.
[10] V.V. Belousov, A.F. Fradkov, K.A. Lukyanov, D.B. Staroverov, K.S. Shakhbazov, A.V. Terskikh, S. Lukyanov, Genetically encoded fluorescent indicator for intracellular hydrogen peroxide, Nat. Methods 3 (2006) 281–286.
[11] M. Eichler, R. Lavi, A. Shainberg, R. Lubart, Flavins are source of visible-light-induced free radical formation in cells, Lasers Surg. Med. 37 (2005) 314–319.
[12] J.W. West, D.E. Patton, T. Scheuer, Y. Wang, A.L. Goldin, W.A. Catterall, A cluster of hydrophobic amino acid residues required for fast Na^+-channel inactivation, Proc. Natl. Acad. Sci. U. S. A. 89 (1992) 10910–10914.
[13] J.C. McPhee, D.S. Ragsdale, T. Scheuer, W.A. Catterall, A critical role for the S4–S5 intracellular loop in domain IV of the sodium channel α-subunit in fast inactivation, J. Biol. Chem. 273 (1998) 1121–1129.
[14] G. Eaholtz, A. Colvin, D. Leonard, C. Taylor, W.A. Catterall, Block of brain sodium channels by peptide mimetics of the isoleucine, phenylalanine, and methionine (IFM) motif from the inactivation gate, J. Gen. Physiol. 113 (1999) 279–293.
[15] W. Ulbricht, Sodium channel inactivation: molecular determinants and modulation, Physiol. Rev. 85 (2005) 1271–1301.
[16] M. Kassmann, A. Hansel, E. Leipold, J. Birkenbeil, S.Q. Lu, T. Hoshi, S.H. Heinemann, Oxidation of multiple methionine residues impairs rapid sodium channel inactivation, Pflugers Arch. 456 (2008) 1085–1095.
[17] M.F. Sheets, D.A. Hanck, Charge immobilization of the voltage sensor in domain IV is independent of sodium channel inactivation, J. Physiol. 563 (2005) 83–93.
[18] R. Haenold, R. Wassef, N. Brot, S. Neugebauer, E. Leipold, S.H. Heinemann, T. Hoshi, Protection of vascular smooth muscle cells by methionine sulfoxide reductase A — role of intracellular localization and substrate availability, Free Radic. Res. 42 (2008) 978–988.
[19] J.S. Trimmer, S.S. Cooperman, S.A. Tomiko, J.Y. Zhou, S.M. Crean, M.B. Boyle, R.G. Kallen, Z.H. Sheng, R.L. Barchi, F.J. Sigworth, R.H. Goodman, W.S. Agnew, G. Mandel, Primary structure and functional expression of a mammalian skeletal muscle sodium channel, Neuron 3 (1989) 33–49.
[20] H. Chen, D. Gordon, S.H. Heinemann, Modulation of cloned skeletal muscle sodium channels by the scorpion toxins Lqh II, Lqh III, and LqhαIT, Pflugers Arch. 439 (2000) 423–432.
[21] J.S. Fan, P. Palade, Perforated patch recording with beta-escin, Pflugers Arch. 436 (1998) 1021–1023.
[22] Y. Higure, Y. Katayama, K. Takeuchi, Y. Ohtubo, K. Yoshii, Lucifer Yellow slows voltage-gated Na^+ current inactivation in a light-dependent manner in mice, J. Physiol. 550 (2003) 159–167.
[23] M.E. Bulina, D.M. Chudakov, O.V. Britanova, Y.G. Yanushevich, D.B. Staroverov, T.V. Chepurnykh, E.M. Merzlyak, M.A. Shkrob, S. Lukyanov, K.A. Lukyanov, A genetically encoded photosensitizer, Nat. Biotechnol. 24 (2006) 95–99.
[24] I. Afanas'ev, ROS and RNS signaling in heart disorders: could antioxidant treatment be successful? Oxidative Med. Cell. Longev. 2011 (2011) 293769.
[25] K.J. Barnham, Colin L. Masters, A.I. Bush, Neurodegenerative diseases and oxidative stress, Nat. Rev. Drug Discov. 3 (2004) 205–214.
[26] M.B. Reid, W.J. Durham, Generation of reactive oxygen and nitrogen species in contracting skeletal muscle: potential impact on aging, Ann. N. Y. Acad. Sci. 959 (2002) 108–116.
[27] R.H. Newman, M.D. Fosbrink, J. Zhang, Genetically encodable fluorescent biosensors for tracking signaling dynamics in living cells, Chem. Rev. 111 (2011) 3614–3666.
[28] A. King, E. Gottlieb, D.G. Brooks, M.P. Murphy, J.L. Dunaief, Mitochondria-derived reactive oxygen species mediate blue light-induced death of retinal pigment epithelial cells, Photochem. Photobiol. Sci. 79 (2004) 470–475.